IIETA International Information and Engineering Technology Association
Advancing the World of Information and Engineering

International Journal of Sustainable Development and Planning
Vol. 17, No. 6, October, 2022, pp. 1693-1698
Journal homepage: http://iieta.org/journals/ijsdp

A Numerical Study on an Integrated Solar Chimney with Latent Heat Thermal Energy Storage in Various Arrangements

Bernardo Buonomo*, Maria Rita Golia, Oronzio Manca, Segio Nardini

Dipartimento di Ingegneria, Università degli Studi della Campania "Luigi Vanvitelli", Via Roma 29, Aversa (CE), Italy

Corresponding Author Email: bernardo.buonomo@unicampania.it

7th int. Conf. AIGE-IIETA and 16th Conf. AIGE—SPECIAL ISSUE

https://doi.org/10.18280/ijsdp.170601

Received: 18 July 2022
Accepted: 3 October 2022

Keywords:
solar chimney, thermal energy storage, energy efficiency, renewable energy system

ABSTRACT

The paper presents a two-dimensional numerical investigation of a solar chimney combined with an absorbing capacity wall in a building's south façade. The analysis was carried out in Aversa (Italy), in July and December, from sunrise to sunset. The chimney is made up of a converging channel, a vertical absorbing wall, and a two-degree angled glass plate. It is 5.0 m tall, while the height of the channel is 4.0 m, with an inlet of 0.34 m and an outlet portion of 0.20 m. A phase change material with metal foam makes up the thermal energy storage system. Four possible configurations are investigated to identify the ideal hybrid system arrangement in terms of thermal performance; the commercial code Ansys-Fluent is used to solve the problem. The results of the thermal energy storage system with metal foam and PCM are provided in terms of liquid fractions, stored energy, and stream function fields, while the ones of the wall temperature distributions in the channel are reported. Thermal and fluid dynamics behaviours are so evaluated to have some useful indications to improve the system.

1. INTRODUCTION

The solar chimney is a feasible passive solar heating and cooling solution that uses clean energy rather than fossil fuels [1, 2]. Solar radiation is used to boost the temperature of the air, and the buoyancy of warm air is used to speed up the airflow through the system [3-5]. The solar chimney is the subject of many studies that have shown how the use of PCM improves its thermal performance, where it is highlighted how the thermal and geometric features of PCMs have a significant impact on overall chimney performance. The outcome of earlier research showed that PCM has a lot of potential for increasing building thermal comfort, extending ventilation duration, enhancing solar chimney power plant electricity output, and extending the generating period [6]. In fact, when phase change materials (PCMs) are combined with a solar chimney, a Latent Heat Thermal Storage System (LHTES) is implemented that can be used in both summer and winter. During the summer, the indoor spaces are refreshed due to the chimney pressing hot air outside, while during the winter, the same system can heat the indoor environments due to the daily storage effect of the PCMs [7, 8].

Kotani et al. [9] and Kaneko et al. [10] proposed an innovative idea of the solar chimney with sodium sulfate decahydrate as PCM for latent heat storage and validated the numerical results with experimental ones. They examined the case of PCM completely melted and PCM did not melt and observed that PCM prolonged the ventilation period in the nighttime if only the PCM was fully melted during the day. According to Sharma et al. [11] integrating the PCM inside the solar chimney can generate a nearly constant average airflow of 155 m^3/h. Amori and Mohammed [12] show that the addition of paraffin wax inside the solar chimney extends the ventilation period after sunset and estimated the thermal efficiency. They studied various air inlet positions and their experimental simulations showed that the solar chimney with a side entrance provided the best thermal performance. Cao et al. [13] noted how air circulation is an essential factor in human productivity and well-being in both residential and commercial structures and they presented and explored a new titled Solar Chimney Ventilator with Phase Change Material integrated with Photovoltaic technology (SCV-PV-PCM). It was observed that the produced power and ventilation capacity of the SCV-PV-PCM is higher than those of the common SCV-PV system.

Numerical experiments of Li and Liu [14] reveal that when the heat flux is less than 500 W/m^2, the system performance decreases rapidly, and there is no significant improvement when the heat flux is greater than 700 W/m^2. Meanwhile, the experimental results show that the melting time of the PCM in the open charging mode is 57% longer than in the closed charging mode, with an 11-hour delay for melting [15], and a 10°C drop in the phase change temperature which results in a 50% reduction in melting time and a 70% increase in solidification time [16]. Tiji et al. [17] demonstrated that finned storage can significantly recover energy dissipation while also increasing the average temperature of the room by 20% compared to a system without fins. The presence of the fins, which create a non-uniform airflow inside the room, increases the rate of flow by roughly 40%. A great way to improve thermal energy storage with PCM is by using metal foam. Many researchers have looked at the benefits of PCM embedded in copper foam in local thermal non-equilibrium (LTNE) [18], and PCM embedded in aluminum foam in local thermal equilibrium (LTE) [19]. Buonomo et al. [20] proved innovatively that the performance of solar chimneys is enhanced using PCM with metal foam.

In this numerical simulation, a two-dimensional prototypal solar chimney system integrated with an absorbent capacity wall of a building's south façade is investigated and both thermal and dynamic behavior are analyzed. The chimney is made up of a converging channel with one vertical absorbing wall and a glass plate that is tilted 2° from the vertical. Behind the absorbing vertical wall is placed the box with phase change material embedded in aluminum metal foam with assigned porosity values and pores per inch (PPI). The box is evaluated in four alternative configurations, each with a different dimension and position along the vertical wall. The governing equations for the transient analysis are the k-ε turbulence model and a two-dimensional airflow model and they are solved with Ansys-Fluent commercial code. The experiments are conducted in Aversa (Italy) in July and December, from dawn to dusk. The outcomes are reported in terms of liquid fractions, energy stored, and stream function fields, as well as wall temperature distributions in the channel.

2. MATHEMATICAL MODEL

The configuration of the solar chimney is depicted in Figure 1, and its geometric parameters are presented in Table 1. It is made up of a channel with an absorbing vertical wall of height L, on which a homogeneous heat source equal to solar irradiance is imposed, and a low-emissivity glass wall inclined to the vertical at an angle equal to 2°. A rectangular box with a thickness of "s" and a height "L/2", as shown in Figures 1(A)-1(C), and “L”, as in Figure 1(D), is placed behind the vertical wall and filled with phase change material embedded in the aluminum foam. b_{max} and b_{min} are the inlet and outlet portions, respectively.

Table 1. Solar chimney dimensions

Dimension	Value
L_b	2.00; 1.00 m
L	4.00 m
s	0.01; 0.02 m
b_{max}	0.34 m
b_{min}	0.20 m

The enthalpy-porosity approach proposed by Voller and Prakash [21] is used to model the solidification and melting of the PCM. During the melting process, there is no noticeable difference between the solid and liquid zones with this approach, but there is a mixed solid-liquid zone. When the material solidifies, the porosity reduces from 1 to 0. This zone is described as a pseudo-porous medium in which the porosity decreases from 1 to 0. A liquid fraction parameter, β, is used to define the mixed region (mushy zone), and its values range from 0 to 1 when the zone is completely solid and liquid, respectively. The value is determined by the temperature of the local, T, and is reported in Eq. (1).

$$\begin{cases} \beta = 0 & \text{for} \quad T < T_{solidus} \\ \beta = \dfrac{T - T_{solidus}}{T_{liquidus} - T_{solidus}} & \text{for} \quad T_{solidus} < T < T_{liquidus} \\ \beta = 1 & \text{for} \quad T > T_{liquidus} \end{cases} \tag{1}$$

The domain is entirely solid when T < $T_{solidus}$ and totally liquid when T > $T_{liquidus}$. When $T_{solidus}$<T<$T_{liquidus}$, melting takes place.

In the present study, the Local Thermal Equilibrium (LTE) is assumed to describe the heat transfer between PCM and metal foam. The Boussinesq approximation is employed to simulate the natural convection of the liquid phase, and the metal foam is modeled as an isotropic and homogeneous porous media.

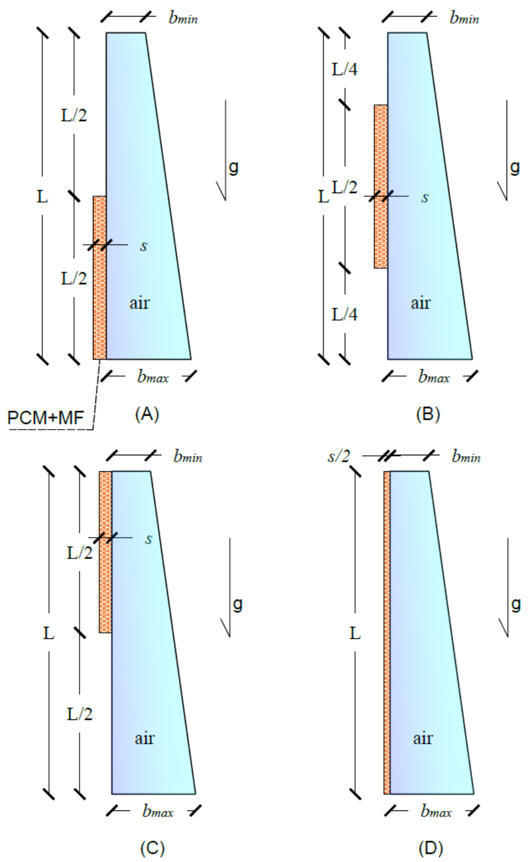

Figure 1. Solar chimney sketch

Since compression work and viscous dissipation are considered to be negligible, the governing equations can be expressed for both the air-zone and the PCM-zone, as described by Buonomo et al. [22]. In addition, a k-ε model is considered, which was first proposed by Launder and Spalding [23] and then by Ayadi et al. [24]. Paraffin wax RT41-43 was chosen as the PCM for this investigation, and its thermal parameters are listed in Table 2 [25]. The aluminum foam with a porosity ε = 0.955 and 20 PPI, was chosen due to its propriety, and parameters [26] are also listed in the same Table 2.

Table 2. Properties of the paraffin wax and aluminum foam [25]

Properties	Paraffin wax 41-43	Aluminum foam
Cp ($J\ kg^{-1}\ K^{-1}$)	2100	2719
ρ ($kg\ m^{-3}$)	829	871
λ ($W\ m^{-1}\ K^{-1}$)	0.21	202.4
μ ($kg\ m^{-1}\ s^{-1}$)	0.0055	-
γ (K^{-1})	0.004	-
h_L (kJ/kg)	228	-
$T_{solidus}$ (K)	314.15	-
$T_{liquidus}$ (K)	316.15	-

The following condition is assumed: the inlet section has ambient temperature and pressure; the PCM is homogenous and isotropic; the heat flux on the heated surface is uniform in each considered hour and changes hour by hour, and the unheated surfaces are adiabatic.

The variation of enthalpy, for the unit of volume, in the PCM is reported in Eq. (2), in which T_0 is equal to 294 K and symbolizes the ambient temperature.

$$\Delta h_{pcm} = \rho_{pcm} h_L \beta + \rho_{pcm} c_v (T - T_0) \tag{2}$$

3. NUMERICAL MODEL

The governing equations are solved by using the Ansys Fluent algorithm and the finite volume approach. Pressure and velocity are coupled using the Semi-Implicit Method for Pressure-Linked Equations (SIMPLE). Meanwhile, the second-order upwind technique is used to discretize convective components in unstable energy and momentum equations. For the open channel with air within, the Surface-to-Surface (S2S) model was chosen as the radiation model and the grey-diffuse model has been employed with Ansys Fluent. The uniform heat production that is transferred on the aluminum plate is τE, where τ is equal to 0.68 and it is the transmittance coefficient of the glass, and E, which is established using a User Define Function, is the Radiant Energy [20]. The choice of mesh is a tradeoff between the quality of the solution and the calculation time; consequently, the sensitivity of the mesh is investigated by examining three computational domains with a total number of cells of 7440 (mesh n.1), 29760 (mesh n.2), and 119040 (mesh n.3). The percentage error is determined using the reference value "h" and the unknown error value "h_x." The grid mesh n.2 is chosen after the sensitivity analysis because it provides the optimum balance between simulation performance and computing time.

4. RESULTS

The results of the thermal energy storage system integrated into the solar chimney are provided in terms of liquid fractions, energy stored, and stream function fields. Otherwise, the results of the wall temperature distributions in the channel are reported. The evolution of liquid fraction is reported in Figure 2 where it can be seen in four cases with different thicknesses of the PCM-MF storage plate, in July and December. When the thickness storage box is s=1 cm the PCM melts and solidifies faster, instead when s=3 cm none of the configurations achieves complete melting during the winter season.

Figure 3(a) shows the energy stored as a function of time, it can be observed that the greater the thickness of the storage plate, the greater will be the accumulated energy, as expected. Figure 3(b) depicts mass flow rate as a function of time. The case with s=3 cm has a mass flow rate in general slightly lower than the case with s=1cm, the most interesting difference is noticed in the final part of the day, after 16:30, during the discharging phase of the storage plate. In fact, s=1 cm discharges earlier, and therefore the curves drop faster, while the trend of the curves with s=3 cm drops more slowly, and it is more stable.

Figure 4 represents the wall temperature profiles along y for s=1 cm in the time range 9:45-18:45 in July. The temperature is constant or grows steadily where the plate of PCM+MF is placed. Looking at Figure 4, at 9:45 the temperature increases and at 12:45 the temperature keeps growing, at 15:45 the temperature is constant in the plate where there is the PCM and starts to decrease on the rest of the wall. Finally, at 18:45, the temperature where there is the plate of PCM+MF remains constant, and it decreases on the rest of the wall quickly. These profiles clearly show how the temperature trends in the wall change concerning the position of the panel with PCM+MF. The best performance is obtained in case D, when the storage plate has the same length as the wall of the solar chimney.

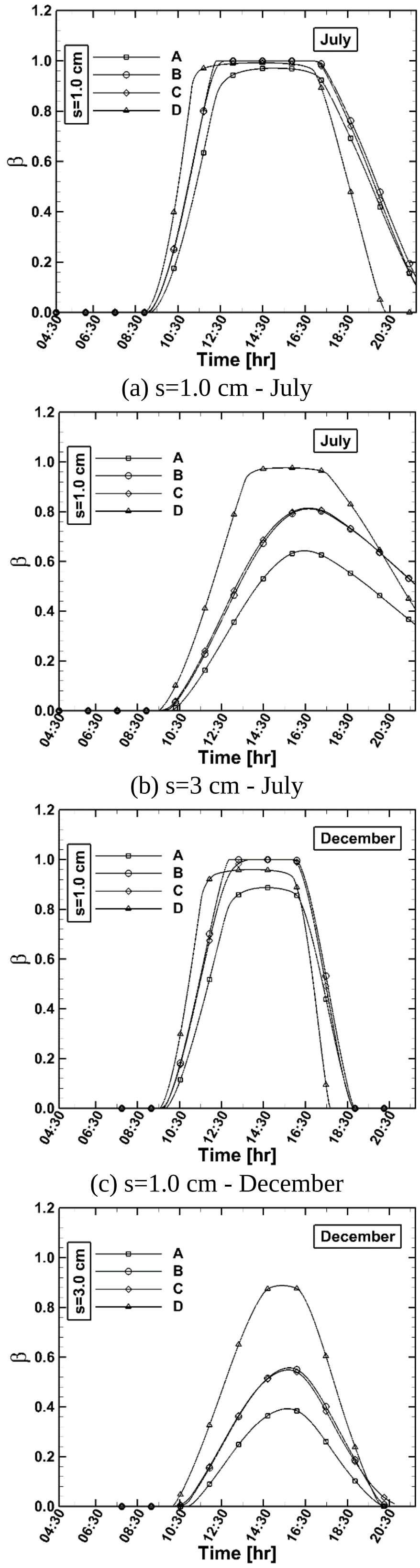

(a) s=1.0 cm - July

(b) s=3 cm - July

(c) s=1.0 cm - December

(d) s=3.0 cm – December

Figure 2. Liquid fraction as a function of time for the configurations (A-D)

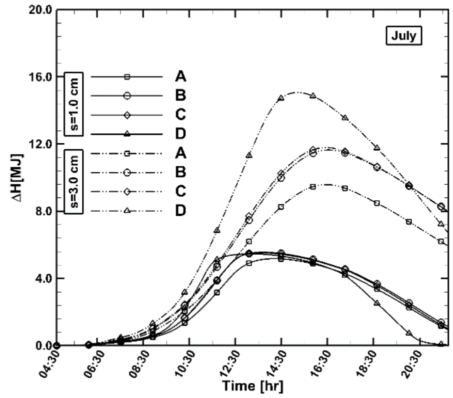

(a) Energy stored as a function of time for s=1.0 cm and 3.0 cm

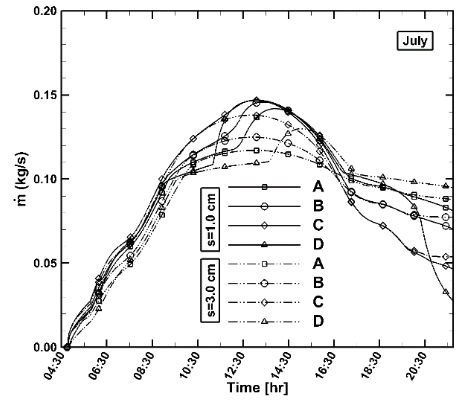

(b) Mass flow rate as a function of time for s=1.0 cm and 3.0 cm

Figure 3. (a) Energy stored as a function of time for s=1.0 cm and 3.0 cm, for various configurations (A-D) in July and (b) Mass flow rate as a function of time for s=1.0 cm and 3.0 cm, for various configurations (A-D) in July

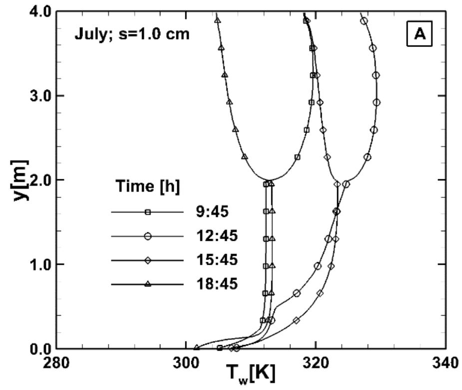

(a) Geometrical configuration A

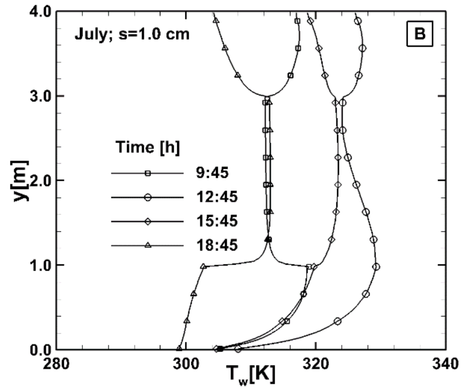

(b) Geometrical configuration B

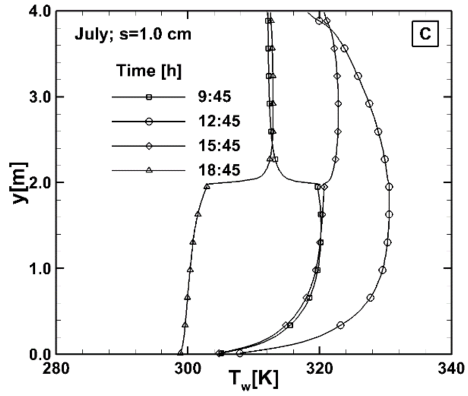

(c) Geometrical configuration C

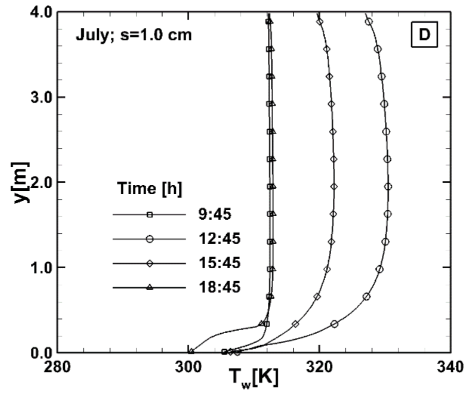

(d) Geometrical configuration D

Figure 4. Wall temperature profiles along y for s=1.0 cm in the time range 9:45-18:45 in July for A-D configurations

5. CONCLUSIONS

It is critical to define a passive system that uses the components of a building to collect, store, and diffuse solar radiation heat without the employment of installation. A solar chimney with latent heat storage is one of the feasible technologies which can be implemented as a passive system. This study intended to evaluate the effects of the various configuration of the storage system in the solar chimney. A high-absorbing plate and a box with phase change material embedded in aluminum metal foam with assigned porosity values and pores per inch (PPI) make up the capacity wall. The box is tested in four distinct configurations, each with a different size and location along the vertical wall. The results show how the wall with and without the PCM+MF plate heats and cools, and how the configuration, thickness, and weather affect the trends of liquid fraction, energy stored and mass flow rate during the day.

ACKNOWLEDGMENT

This research was funded by Ministero dell'Istruzione, dell' Università e della Ricerca (MIUR), grant number PRIN-2017F7KZWS and by Università degli Studi della Campania "Luigi Vanvitelli" with the grant number D.R. n. 138 under NanoTES project - V: ALERE program 2020.

REFERENCES

[1] Schelbach, S. (2016). Developing a method to improve

the energy efficiency of modern buildings by using traditional passive concepts of resource efficiency and climate adaptation. International Journal of Sustainable Development and Planning, 11(1): 23-38. https://doi.org/10.2495/SDP-V11-N1-23-38

[2] Cruz, A.S., de Carvalho, R.S., da Cunha, E.G. (2020). Passive house alternative proposal for the Brazilian Bioclimatic Zone 8. International Journal of Sustainable Development and Planning, 15(6): 827-833. https://doi.org/10.18280/ijsdp.150605

[3] Buonomo, B., Manca, O., Nardini, S., Romano, P. (2013). Thermal and fluid dynamic analysis of solar chimney building systems. International Journal of Heat and Technology, 31(2): 119-126. https://doi.org/10.18280/ijht.310216

[4] Cirillo, L., Di Ronza, D., Fardella, V., Manca, O., Nardini, S. (2015). Numerical and experimental investigations on a solar chimney integrated in a building façade. International Journal of Heat and Technology, 33(4): 246-254. https://doi.org/10.18280/ijht.330433

[5] Ghernaout, B., Bouabdallah, S., Attia, M.E.H., Arıcı, M., Driss, Z. (2020). Parametric study of the airflow structure in a solar chimney. International Journal of Heat and Technology, 38(2): 285-292. https://doi.org/10.18280/ijht.380202

[6] Omara, A.A.M., Mohammed, H.A., Al Rikabi, I.J., Abuelnour, M.A., Abuelnuor, A.A.A. (2021) Performance improvement of solar chimneys using phase change materials: A review. Solar Energy, 228: 68-88. https://doi.org/10.1016/j.solener.2021.09.037

[7] Cabeza, L.F. (2021). Advances in Thermal Energy Storage Systems: Methods and Applications. Elsevier.

[8] Dincer, I., Rosen, M.A. (2011). Thermal Energy Storage: Systems and Applications. 2nd ed., Wiley, New York.

[9] Kotani, H., Sharma, S.D., Kaneko, Y., Yamanaka, T., Sagara, K. (2005). Development of solar chimney with built-in latent heat storage material for natural ventilation. International Journal of Green Energy, 4(3): 313-324. https://doi.org/10.1080/15435070701332120

[10] Kaneko, Y., Sagara, K., Yamanaka, T., Kotani, H. (2006). Ventilation performance of solar chimney with build-in latent heat storage. https://www.researchgate.net/publication/265989559_Ventilation_performance_of_solar_chimney_with_built-in_latent_heat_storage, accessed on Apr. 20, 2022.

[11] Sharma, S.D., Kotani, H., Kaneko, Y., Yamanaka, T., Sagara, K. (2007). Design, development of a solar chimney with built-in latent heat storage material for natural ventilation. International Journal of Green Energy, 4(3): 313-324. https://doi.org/10.1080/15435070701332120

[12] Amori, K.E., Mohammed, S.W. (2012). Experimental and numerical studies of solar chimney for natural ventilation in Iraq. Energy and Buildings, 47: 450-457. https://doi.org/10.1016/j.enbuild.2011.12.014

[13] Cao, Y., Sinaga, N., Pourhedayat, S., Dizaji, H.S. (2021). Innovative integration of solar chimney ventilator, solar panel and phase change material; under real transient weather condition of Hong Kong through different months. Renewable Energy, 174: 865-878. https://doi.org/10.1016/j.renene.2021.04.146

[14] Li, Y., Liu, S. (2014). Numerical study on thermal behaviors of a solar chimney incorporated with PCM. Energy and Buildings, 80: 406-414. https://doi.org/10.1016/j.enbuild.2014.05.043

[15] Liu, S., Li, Y. (2015). An experimental study on the thermal performance of a solar chimney without and with PCM. Renewable Energy, 81: 338-346. https://doi.org/10.1016/j.renene.2015.03.054

[16] Li, Y., Liu, S., Lu, J. (2017). Effects of various parameters of a PCM on thermal performance of a solar chimney. Applied Thermal Engineering, 127: 1119-1131. https://doi.org/10.1016/j.applthermaleng.2017.08.087

[17] Tiji, M.E., Eisapour, M., Yousefzadeh, R., Azadian, M., Talebizadehsardari, P. (2020). A numerical study of a PCM-based passive solar chimney with a finned absorber. Journal of Building Engineering, 32: 101516. https://doi.org/10.1016/j.jobe.2020.101516

[18] Zhang, P., Meng, Z., Zhu, H., Wang, Y., Peng, S. (2015). Experimental and numerical study of heat transfer characteristics of a paraffin/metal foam composite PCM. Energy Procedia, 75: 3091-3097. https://doi.org/10.1016/j.egypro.2015.07.637

[19] Buonomo, B., Celik, H., Ercole, D., Manca, O., Mobedi, M. (2019). Numerical study on latent thermal energy storage systems with aluminum foam in local thermal equilibrium. Applied Thermal Engineering, 159: 113980. https://doi.org/10.1016/j.applthermaleng.2019.113980

[20] Buonomo, B., Capasso, L., Diana, A., Manca, O., Nardini, S. (2019). A numerical analysis on a solar chimney with an integrated latent heat thermal energy storage. AIP Conference Proceedings, 2191: 020029. https://doi.org/10.1063/1.5138762

[21] Voller, V.R., Prakash, C. (1987). A fixed grid numerical modelling methodology for convection-diffusion mushy region phase-change problems. International Journal of Heat and Mass Transfer, 30(8): 1709-1719. https://doi.org/ 10.1016/0017-9310(87)90317-6

[22] Buonomo, B., Capasso, L., Manca, O., Menale, F., Nardini, S. (2020). A numerical analysis on a solar chimney with an integrated thermal energy storage with phase change material in metal foam. E3S Web of Conferences, 197: 08001. https://doi.org/10.1051/e3sconf/202019708001

[23] Launder, B.E., Spalding, D.B. (1974). The numerical computation of turbulent flows. Computer Methods in Applied Mechanics and Engineering, 3(2): 269-289. https://doi.org/10.1016/0045-7825(74)90029-2

[24] Ayadi, A., Driss, Z., Bouabidi, A., Abid, M.S. (2017). Experimental and numerical study of the impact of the collector roof inclination on the performance of a solar chimney power plant. Energy and Buildings, 139: 263-276. https://doi.org/10.1016/j.enbuild.2017.01.047

[25] Xamán, J., Vargas-López, R., Gijón-Rivera, M., Zavala-Guillén, I., Jiménez, M.J., Arce, J. (2019). Transient thermal analysis of a solar chimney for buildings with three different types of absorbing materials: Copper plate/PCM/concrete wall. Renewable Energy, 136: 139-58. https://doi.org/10.1016/j.renene.2018.12.106

[26] Yang, J., Du, X., Yang, L., Yang, Y. (2013). Numerical analysis on the thermal behavior of high temperature latent heat thermal energy storage system. Solar Energy, 98(PC): 543-552. https://doi.org/10.1016/j.solener.2013.10.028

NOMENCLATURE

b_{max}	width of the inlet section, m
b_{min}	width of the outlet section, m
Cp	specific heat, J. kg^{-1}. K^{-1}
g	gravity acceleration, m.s^{-2}
L	height of the chimney, m
L_h	height of the thermal energy storage, m
h	specific enthalpy, kJ kg^{-1}
H	enthalpy, J
h_L	latent heat of PCM, J kg^{-1}
s	Thickness, m
$T_{solidus}$	solidus temperature, K
$T_{liquidus}$	liquidus temperature, K
T_{wall}	wall temperature, K
y	coordinate along the heated wall, m

Greek symbols

β	liquid fraction
γ	thermal expansion, K^{-1}
ε	porosity
λ	thermal conductivity, W. m^{-1}. K^{-1}
μ	viscosity, kg. m^{-1}. s^{-1}
ρ	density, kg. m^{-3}
ω	pore size, PPI

Subscripts

mf	Metal foam
pcm	Phase change material